J Therm Anal Calorim (2012) 110:755–764
DOI 10.1007/s10973-011-1976-9

Thermoanalytical investigations on the solid-state synthesis of Sr-doped praseodymium alkaline-earth cobalt oxides

Edoardo Magnone · Jong Pyo Kim · Jung Hoon Park

Received: 11 July 2011 / Accepted: 5 October 2011 / Published online: 22 October 2011

Abstract In this study, the formation and characteristics of Sr-doped praseodymium alkaline-earth cobalt oxide were studied as a function of the strontium content (x). $PrBa_{1-x}Sr_xCo_2O_{5+d}$ ceramics with $x = 0.0$, 1/16, 1/8, 1/4, and 1/2.5 were prepared by solid-state reaction method from Pr_6O_{11}, $BaCO_3$, $SrCO_3$, and Co_3O_4. The solid-state reaction mechanisms were analyzed by differential thermal analysis (DTA) and thermogravimetry (TG) techniques to characterize properly the distinct thermal events occurring during synthesis of layered perovskite-type $PrBa_{1-x}Sr_xCo_2O_{5+d}$ oxides. The X-ray diffraction (XRD) results were used to assist the interpretation of DTA–TG analyses. The TG, DTA, and XRD results for the mixtures showed that the solid-state reaction between precursors was completed in a temperature range between 800 and 1000 °C. The strong influence of strontium contents (x) on the solid-state reaction temperatures and $PrBa_{1-x}Sr_xCo_2O_{5+d}$ structure was found.

Keywords Layered perovskite-type $PrBa_{1-x}Sr_xCo_2O_{5+d}$ oxides · Thermoanalytical investigations · XRD · Reactivity of solids · Solid-state reaction

E. Magnone (✉) · J. H. Park (✉)
Greenhouse Gas Research Center, Korea Institute of Energy Research, 71-2, Jang-dong, Yuseong-gu, Daejeon 305-343, Republic of Korea
e-mail: magnone.edoardo@gmail.com

J. H. Park
e-mail: pjhoon@kier.re.kr

J. P. Kim
Department of Chemical Engineering, Chungnam National University, 220, Gung-dong Yuseong-gu, Daejeon 305-764, Republic of Korea

Introduction

Perovskite oxides represent a prominent of advanced compounds involved in many areas of science and technology [1–3]. Mixed conducting oxide that exhibits both electron and oxygen ion conduction are attractive materials because of their various applications such as solid oxide fuel cell (SOFC) cathodes and dense ceramic membrane for oxygen separation [4]. Among the various oxides used, a layered group of cobalt-based perovskites with formula $REEBaCo_2O_{5+d}$ (REE = Rare earth element) has recently captured the interest of researchers coming from a number of disciplines because of their unique magnetic [5–10] and electrochemical properties [4, 11–15].

The most common technique for the production of $REEBaCo_2O_{5+d}$ powders is the conventional high-temperature solid-state reaction method of physical mixture of REE_2O_3—or REE_6O_{11} in the case of Praseodymium—and Co_3O_4 oxides with carbonates $BaCO_3$ in stoichiometric ratio to obtain the chosen layered perovskite compound [4–15]. In the recent literature there is a multitude of investigations concerning the magnetic, structure, and the electrochemical properties of $REEBaCo_2O_{5+d}$ oxygen-deficient perovskite compounds [4–15] but reports on solid-state reaction mechanisms are rather rarely published. Understanding the solid-state reaction mechanisms is necessary for improving the knowledge of materials science and control of synthesis process.

In this research, a series of layered perovskite-type $PrBa_{1-x}Sr_xCo_2O_{5+d}$ samples ($x = 0.0$, 1/16, 1/8, 1/4, and 1/2.5) was examined. In particular, we have examined the decomposition and sub-sequent reactions of $PrBa_{1-x}Sr_xCo_2O_{5+d}$ precursors as a function of the strontium content (x) and annealing temperature using differential

thermal analysis (DTA), thermogravimetric analysis (TG), and X-ray diffraction (XRD) techniques.

Experimental

Samples with different strontium content (x) were prepared by classical ceramic method by solid-state reaction from high purity oxides and carbonates. Phase transformations of the quaternary ($x = 1/16$, 1/8, 1/4, and 1/2.5) mixtures of Pr_6O_{11}, $BaCO_3$, $SrCO_3$, and Co_3O_4 powders were examined using DTA/TG in a dynamic (20 mL/min) atmosphere of air. Pr_6O_{11}, $BaCO_3$, $SrCO_3$, and Co_3O_4 were used as starting precursor materials where the general reaction of formation of $PrBa_{1-x}Sr_xCo_2O_{5+d}$ oxide can be written as follows:

$$Pr_6O_{11} + 6(1-x)\ BaCO_3 + 6x\ SrCO_3 + 4\ Co_3O_4 \rightarrow 6\ PrBa_{1-x}Sr_xCo_2O_{5+d} + 6(1-x)\ CO_2 + [15 - 12(1-x)]/2\ O_2 \quad (1)$$

The starting mixtures containing basic oxides and carbonates were homogenized in an agate mortar for 1 h. After mixing the appropriate amounts of starting ternary and quaternary powders, all dried mixtures of precursors were subject to differential thermal analysis (DTA) and thermogravimetric analysis (TG). DTA and TG were carried out using a Thermal Analysis-SDT2960 (TA Instruments, U.S.A.) in air flow (100 mL/min) at temperature range 20–1200 °C. The mass of sample in all runs was about 60 mg. The reference material was γ-Al_2O_3. The heating and cooling rate was 5 °C/min. All experiments were performed under atmospheric pressure where an open alumina crucible with 5.5 mm inner diameter and 4.1 mm high was used as a sample container.

Moreover, phase transformations of some representative binary (i.e., $Pr_6O_{11} + BaCO_3$; $Pr_6O_{11} + SrCO_3$; $BaCO_3 + SrCO_3$) and ternary (i.e., $Pr_6O_{11} + BaCO_3 + Co_3O_4$), mixtures, and the corresponding thermal events of each component (i.e., Pr_6O_{11}; $BaCO_3$; $SrCO_3$; Co_3O_4), were also examined using DTA/TG. The starting single raw materials (Pr_6O_{11}, $BaCO_3$, $SrCO_3$ and Co_3O_4), binary ($PrBaO_3$, $PrSrO_3$, $Ba_{0.5}Sr_{0.5}CO_3$) and ternary ($x = 0.0$) mixtures were studied by thermal analysis in the same condition of quaternary ($x = 1/16$, 1/8, 1/4, and 1/2.5) mixture. In particular, to prepare $PrBaO_3$, $PrSrO_3$, and $Ba_{0.5}Sr_{0.5}CO_3$ solid solution the same following solid-state synthesis procedure was performed:

$$Pr_6O_{11} + 6\ BaCO_3 + 1/2\ O_2 \rightarrow 6\ PrBaO_3 + 6\ CO_2 \quad (2)$$

$$Pr_6O_{11} + 6\ SrCO_3 + 1/2\ O_2 \rightarrow 6\ PrSrO_3 + 6\ CO_2 \quad (3)$$

$$SrCO_3 + BaCO_3 \rightarrow 2Ba_{0.5}Sr_{0.5}CO_3 \quad (4)$$

From the thermoanalytical curves of individual component, binary, ternary, and quaternary mixture, the temperature ranges in which the chemical reactions and phase transformations occurred have been determined. Moreover, representative precursor mixtures were calcined at three chosen temperatures (800, 1000, and 1200 °C) for 2 h. Cooled samples were subject to X-ray diffraction (XRD) analysis ($CuK_\alpha = 1.5405$ Å) in the Bragg angle range from 20 to 80°. X-ray powder diffraction measurements (Rigaku Co Model D/Max 2200-Ultimaplus, Japan) were performed with a scan step of 0.05° at room temperature. The XRD results were used to assist the interpretation of thermoanalytical results.

Results

Thermal events of the single components and binary mixtures

Pr_6O_{11} single component

The thermal behavior of Pr_6O_{11} single component, where 1/3 of the cations are in the trivalent state [16], was investigated using DTA measurement over the temperature range above 1000 °C. The DTA curve recorded for Pr_6O_{11} at 5 °C/min in a dynamic atmosphere of air (20 mL/min) are shown in Fig. 1a. The figure indicates that decomposition proceeds at last in three stages. This observation is in agreement with the well-reported fact that the praseodymium ions are available in multi-oxidation states of Pr^{3+} and Pr^{4+} in the mixed oxide Pr_6O_{11}, namely Pr_2O_3 $4PrO_2$ [16]. The DTA curve is a result of two endothermic events at relatively low temperature; 292 and 469 °C. The corresponding third broad DTA peak at about 870 °C is bigger than the first two. The first stage in the temperature range from 200 to 500 °C is attributed to the decomposition of praseodymium sesquioxide to praseodymium (III) oxide:

$$Pr_6O_{11} \rightarrow 3\ Pr_2O_3 + O_2 \quad (5)$$

Thermal reduction of Pr_2O_3 to Pr_2O_{3-d}, as also reported in literature, usually occurs in multi-steps [17]:

$$Pr_2O_3 \rightarrow Pr_2O_{3-d} + d/2\ O_2 \quad (6)$$

The evolution of oxygen gas in Eq. 6 during decomposition of the Pr_2O_3 was observed at ~750 °C [17]. For the purpose of the present description, the last stage in the temperature range above 500–1000 °C is related to a slow oxygen evolution with rearrangement of the Pr rich phase. These results are in good accord with recently reported experiments [17–19], while these results differ significantly from results presented in Ref. [20] where the authors

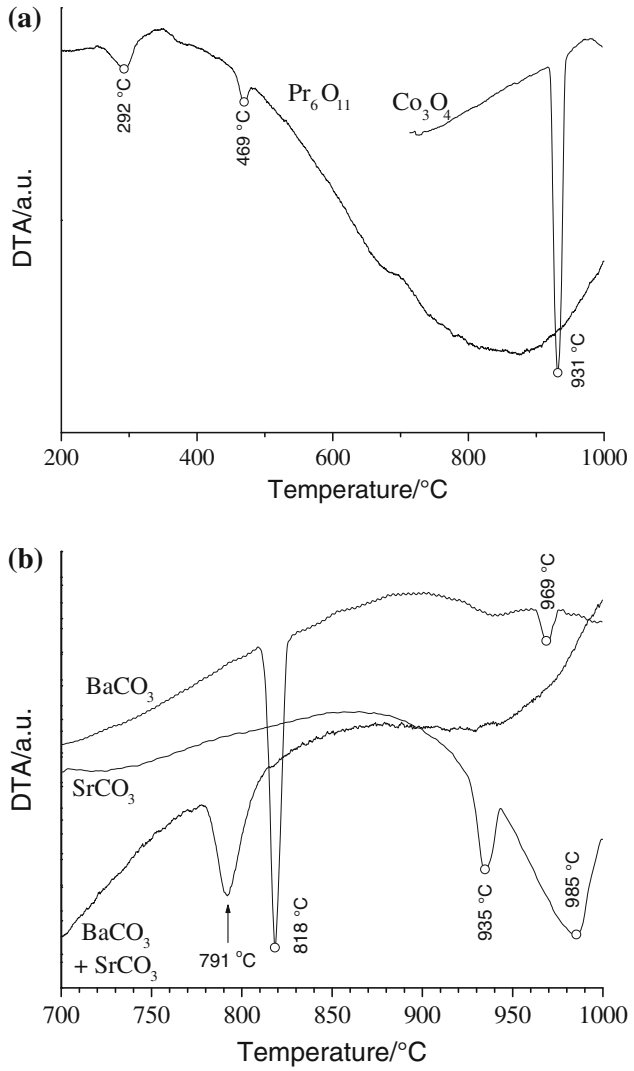

Fig. 1 DTA curves in the heating (5 °C/min) for the raw oxide precursors (Pr_6O_{11} and Co_3O_4) (**a**) and for the raw carbonate precursors ($BaCO_3$ and $SrCO_3$) and for the $BaCO_3$–$SrCO_3$ binary mixture (**b**)

observed a decomposition of Pr_6O_{11}–Pr_2O_3 at about 770 °C. This difference may be the effect of different sample preparation methods or different sample size [21].

Co_3O_4 single component

For reference, a thermal analysis of pure Co_3O_4 single component was carried out. Figure 1a shows the typical DTA curve of Co_3O_4 single component between 700 and 1000 °C. The DTA curve for this component indicates a single exothermic event centered at 931 °C in good accord with literature findings [22, 23]. According to the previous report [22], Co_3O_4 is the thermodynamically stable form of cobalt oxide under atmospheric air below 900 °C and recently Tang et al. [24] have shown that the CoO may be obtained by thermal decomposition of Co_3O_4 at 950 °C. In conclusion, the single exothermic event at 931 °C (Fig. 1a) is ascribable, without any doubt, to the reduction of Co_3O_4 to CoO with liberation of oxygen according to the reaction:

$$Co_3O_4 \rightarrow 3CoO + 1/2O_2 \quad (7)$$

$BaCO_3$ and $SrCO_3$ single components

Figure 1b shows representative DTA curves obtained for $BaCO_3$ single component. As shown clearly in the Fig. 1b, on heating, the $BaCO_3$ sample undergoes two polymorphic transformations which take place below its decomposition temperature [25, 26]. The event at 818 °C is the first transformation from orthorhombic to hexagonal structure:

$$\gamma BaCO_3 \rightarrow \beta BaCO_3 \quad (8)$$

At higher temperature a second polymorphic transformations from hexagonal into cubic structure takes place at 969 °C. At the end, $BaCO_3$ started to decompose between 1361 and 1350 °C [25].

Furthermore, Fig. 1b also shows the differential temperature signals measured as a function of the temperature for $SrCO_3$ single component. In particular, it is shown that the orthorhombic–hexagonal transition take place at 935 °C, in really good agreement with the results already published [26]. The endothermic peak at about 935 °C in the DTA curve corresponds to the polymorphic transformation:

$$\gamma SrCO_3 \rightarrow \beta SrCO_3 \quad (9)$$

The thermal decompositions of carbonates have been very amply described and extensively discussed elsewhere [25–27]. As it can be seen, within experimental error, there is good agreement between our experimental results and the results of the above cited authors.

Pr_6O_{11}–$BaCO_3$ system

In order to better understand the solid-state reaction between the oxide and carbonates in the starting Pr_6O_{11}, $BaCO_3$, $SrCO_3$, and Co_3O_4 mixture, the mechanism of reaction between Pr_6O_{11} and $BaCO_3$ was also investigated by DTA. Figure 2 shows DTA curves for Pr_6O_{11}–$BaCO_3$ mixtures as reported in Eq. 2. Overall, the figure shows that both endothermic events at ~306 and 470 °C associated with Pr_6O_{11} component are constant within the errors of the measurements. As a consequence, both these temperatures are related to a constant mechanism associated to Pr_6O_{11} during the mixture reaction with $BaCO_3$. On the contrary, the endothermic peaks associated with $BaCO_3$ show that the two-stage transformation process, from orthorhombic to hexagonal ($T \cong 831$ °C) and from hexagonal to cubic structure ($T \cong 1000$ °C), shifts to higher temperatures in

the Pr_6O_{11}–$BaCO_3$ mixture system. One explanation may be that at about 830 °C $BaCO_3$ was decomposed and the formation of $PrBaO_3$ began at lower temperature than single component decomposition in good accord with other published articles [28]. In particular, these authors obtained a single phase $BaPr_{0.9}Y_{0.1}O_3$ by low temperature combustion process at 850 °C.

Pr_6O_{11}–$SrCO_3$ system

A mixed Pr_6O_{11} and $SrCO_3$ powder (see Eq. 3) has been analyzed by DTA in the temperature range of 25–1200 °C. Considering the DTA curve reported in Fig. 2, the results obtained show that $SrCO_3$ have a little influence on the decomposition of praseodymium sesquioxide to praseodymium (III) oxide but, in other hand, the interval temperature between the first orthorhombic–hexagonal transition and second endothermic peaks for the $SrCO_3$ in the present powder Pr_6O_{11}–$SrCO_3$ mixture is about 40 °C. In fact, the results of this study suggest that the orthorhombic–hexagonal phase transformation peak associate at $SrCO_3$ (Eq. 9) shifts to higher temperatures in a Pr_6O_{11}–$SrCO_3$ mixture system.

Supplementary evidence based on X-ray structural analysis is presented in Fig. 3a, b as further evidence supporting the suggested origins for DTA peaks in Fig. 2 for Pr_6O_{11}–$BaCO_3$ and Pr_6O_{11}–$SrCO_3$ systems, respectively. We have investigated the phase transition in the Pr_6O_{11}–$BaCO_3$ and Pr_6O_{11}–$SrCO_3$ systems at 800 °C by powder XRD. Figure 3 shows the XRD pattern of reacted Pr_6O_{11}–$BaCO_3$ (Eq. 2) and Pr_6O_{11}–$SrCO_3$ mixtures (Eq. 3) at 800 °C in static air atmosphere (1 h). A clear $BaPrO_3$ phase is observed in Fig. 3a, whereas at the same calcining temperature of 800 °C, room temperature XRD patterns did not show any significant peaks corresponding to $SrPrO_3$-like phase (Fig. 3b). It may be concluded from these results that Pr_6O_{11}–$BaCO_3$ powder mixture reacted at a lower temperature than the Pr_6O_{11}–$SrCO_3$ system. The phases revealed by XRD and DTA were in good agreement with those found in previous studies [28–30].

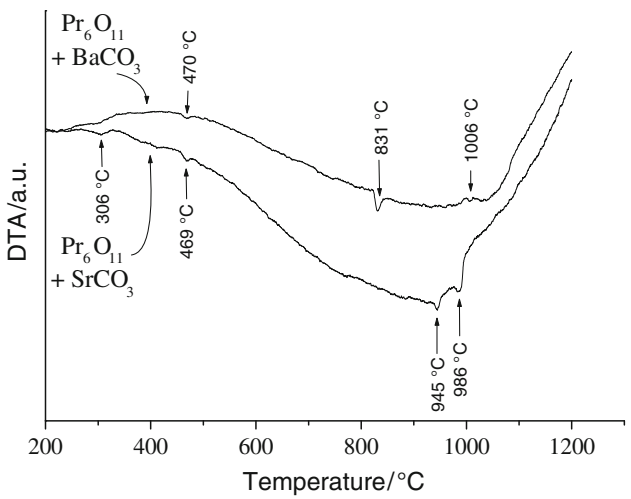

Fig. 2 DTA curves in the heating (5 °C/min) for the Pr_6O_{11}–$BaCO_3$ and Pr_6O_{11}–$SrCO_3$ binary mixtures

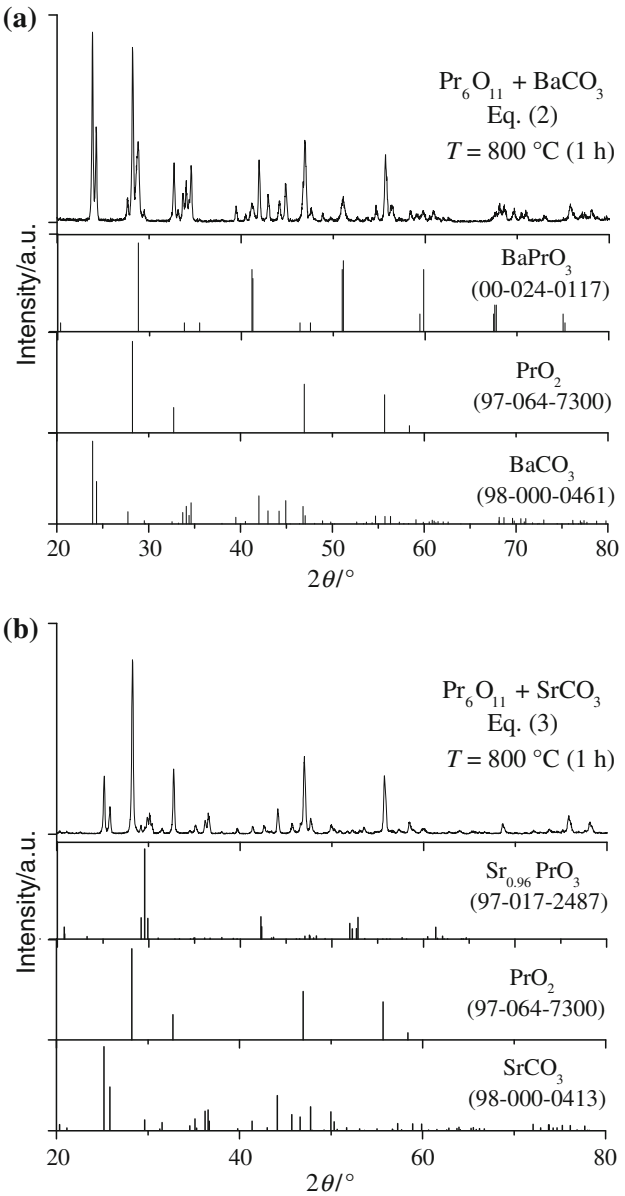

Fig. 3 XRD studies indicating the crystallographic phase evolution for the Pr_6O_{11}–$BaCO_3$ (**a**) and Pr_6O_{11}–$SrCO_3$ (**b**) binary mixtures calcinated in air at 800 °C for 1 h. Data were collected at room temperature. The vertical lines indicate the Bragg peak positions for $BaPrO_3$ (JCPDS#00-024-0117), $Sr_{0.96}PrO_3$ (JCPDS#97-017-2487), PrO_2 (JCPDS#97-064-7300), $BaCO_3$ (JCPDS#98-000-0461), and $SrCO_3$ (JCPDS#98-000-0413)

$BaCO_3$–$SrCO_3$ system

The DTA curve is shown in Fig. 1b while the Table 1 shows the results of our measurement on the $BaCO_3$ + $SrCO_3$ system. In accord with literature data [26], an endothermic peak at 791 °C indicates the first transformation from orthorhombic to hexagonal structure of $Ba_{1-x}Sr_xCO_3$ solid solution ($x = 0.5$) as reported in Eq. 4. This peak shifts toward lower temperature in comparison with pure $BaCO_3$ or $SrCO_3$.

The phase transformation in the system $BaCO_3$–$SrCO_3$, which form a complete solid solution, has been investigated by a number of experimental techniques, including DTA by Weinbruch et al. [26]. Their results showed that the orthorhombic carbonate $BaCO_3$ and $SrCO_3$ transform into a hexagonal structure at 793 and 924 °C, respectively, and a minimum is evident for the same transformation at a composition near 40% Sr-doped $BaCO_3$ with a peak temperature at ~794 °C. On the basis of our analysis of the $Ba_{1-x}Sr_xCO_3$ solid solution mixtures it can be concluded that, in first approximation, the absence of $SrCO_3$ in the ternary mixture (Sr = 0) or different $SrCO_3$ content in the quaternary mixtures (x = 1/16, 1/8, 1/4, and 1/2.5) may influence the solid-state reaction between the Pr_6O_{11}, $BaCO_3$, and Co_3O_4 powders.

Thermal events of the ternary ($x = 0.0$) and quaternary mixtures (x = 1/16, 1/8, 1/4, and 1/2.5)

Undoped praseodymium alkaline-earth cobalt oxides

The curves of mass loss to temperature (TG) and first order of differentiation curve of mass loss (DTG) of the Pr_6O_{11}, $BaCO_3$, and Co_3O_4 mixture ($x = 0$) were obtained. The solid-state reaction between Pr_6O_{11}, $BaCO_3$, and Co_3O_4 to undoped praseodymium alkaline-earth cobalt oxides proceeds via a complex process. In Fig. 4a, three weight loss steps on the TG curve were found. First weight loss, in the temperature range between 245 and 293 °C, was ascribed to the decomposition of praseodymium sesquioxide to praseodymium (III) oxide (Eq. 5), which is supported by the DTA result shown in Fig. 1. The following pronounced weight loss stage, from about 617–1000 °C, corresponding to about 8 wt% weight loss, is likely due to the following reactions: two-stage transformation $BaCO_3$ process (Eq. 8) and reduction of Pr_2O_3 and Co_3O_4 to Pr_2O_{3-d}//PrO_2 and CoO (Eqs. 6, 7), respectively. The inflexions in the DTG curves also show multiple peaks. The first one corresponds to Eq. 5 of the Pr_6O_{11} compounds. The several other DTG peaks in the temperature range 300−500 and at 843−908 °C are recorded but without drawing conclusions. We consider that the last DTG peak at 940 °C can be attributed to the reduction of Co_3O_4 (Eq. 7).

As regards DTA peaks (Fig. 4b), the endothermic peaks due to the sequentially Pr_6O_{11} decomposition are evident at 274, 478, and 491 °C. Moreover, as seen in the inset of Fig. 4b, synthesis processes of $PrBaCo_2O_{5+d}$ at high temperature are complex multistage process where each stage is composed of several endothermic events as following: 780, 818, 893, 908, 940, and 964 °C. We observe that, in

Table 1 Transition temperature in the $BaCO_3$ + $SrCO_3$ system

Composition	Orthorhombic–hexagonal transition		Ref.
	Tangent temperature/°C	Peak temperature/°C	
$BaCO_3$	809	818	This study
$BaCO_3$	793	808	[26]
$Ba_{0.5}Sr_{0.5}CO_3$	780	791	This study
$Ba_{0.5}Sr_{0.5}CO_3$	783	794	[26]
$SrCO_3$	927	935	This study
$SrCO_3$	924	935	[26]

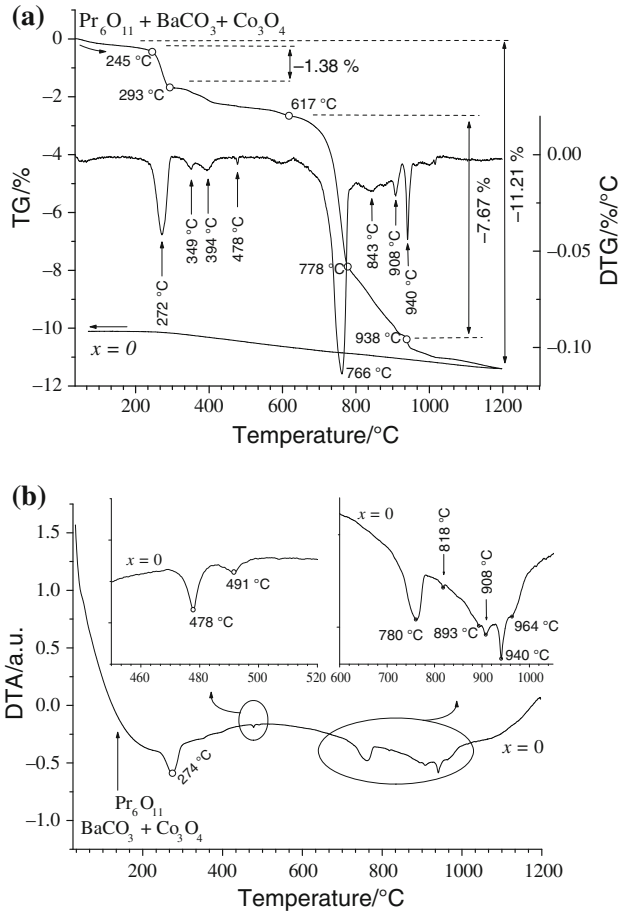

Fig. 4 Combined TG/DTG (**a**) and DTA curves (**b**) obtained from the ternary mixtures ($x = 0$) of Pr_6O_{11}, $BaCO_3$, and Co_3O_4 powders

the first approximation, these thermal events (780–964 °C) correspond to decomposition of single components, binary and/or ternary system reaction in the Pr_6O_{11}, $BaCO_3$, and Co_3O_4 mixture as demonstrated above.

Sr-doped praseodymium alkaline-earth cobalt oxides

The $PrBa_{1-x}Sr_xCo_2O_{5+d}$ ceramic were obtained by solid-state reaction from quaternary raw mixtures with various strontium content ($x = 1/16$, 1/8, 1/4, and 1/2.5) and studied by TG. In Fig. 5a, the TG curve showed a total weight loss of about −11/12% up to 1200 °C, which is due to the evolution of oxygen and carbon compound as CO or CO_2. Solid-state reaction of all the mixtures gives almost the same temperature of about 800 °C, but at different completion temperatures in the range of 800–1000 °C, depends on the strontium content (x). In particular, the mass loss measured up to 1200 °C amounts to −11.39, 11.31, 11.37, 11.73% of the $x = 1/16$, 1/8, 1/4, and 1/2.5 samples, respectively, while it is only −11.21% of the ternary mixture (see Fig. 4a). It is very difficult to detect when more than one reaction is occurring simultaneously from a simple inspection of experimental TG curves and it is also well known that DTG curve offers a possibility to find the inflexion point in the complex TG curve and then separate—if any—the single reaction steeps. For these reasons, in this study, we also report the results of DTG curves for the quaternary mixtures ($x = 1/16$, 1/8, 1/4, and 1/2.5) with the aim to understand the complex interactions that occur between all single components in a mixture of oxides (Pr_6O_{11}, Co_3O_4) and carbonates ($BaCO_3$, $SrCO_3$) [31, 32]. A comparison of DTG curves measured at below 600 °C shows small differences as reported in Fig. 5b. At more high temperature, it is found that the DTG peak for high-strontium content ($x = 1/2.5$) at 922 °C splits into two peaks at low strontium content ($x = 1/16$) at temperatures around 915 and 942 °C. The last DTA peak, appearing at 970 °C in the $x = 1/16$ mixture, has to be assigned to the second polymorphic transformations from hexagonal into cubic structure of $BaCO_3$ phase in the quaternary mixture. DTG peak intensity decreased with increasing strontium content (x). Moreover, it can be seen that the DTG peak shifts at lower temperatures by increasing the strontium content (x) in the starting mixture. These results are in good agreement with those mentioned in the above section.

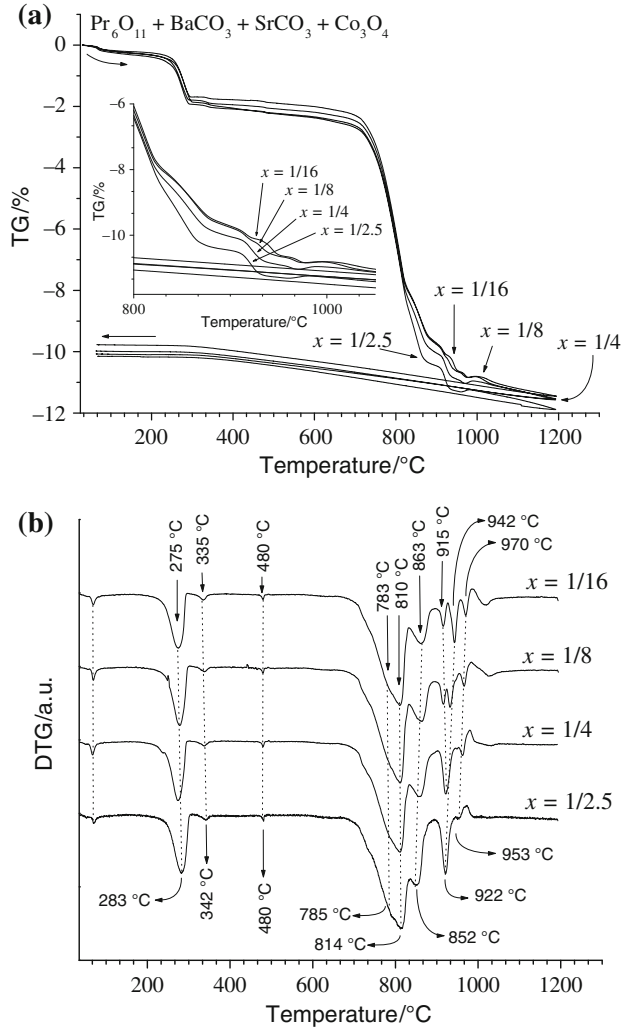

Fig. 5 TG (**a**) and DTG curves (**b**) obtained from the quaternary mixtures ($x = 1/16$, 1/8, 1/4, and 1/2.5) of Pr_6O_{11}, $BaCO_3$, $SrCO_3$, and Co_3O_4 powders

Figure 6 shows a comparison of quantitative evolution rate DTA data for four different powder mixtures with various strontium content ($x = 1/16$, 1/8, 1/4, and 1/2.5). It can be seen that single peak at 817 °C at low strontium content ($1/16 < x < 1/8$) split into two overlapping peaks at 797 and 822 °C as the strontium content was increased ($x > 1/4$). The weak peak at about 870 °C, which exhibits a relatively small shift toward lower temperatures with increasing strontium-dopant content (x) in the mixtures, is isolated from the other peaks. Moreover, Fig. 6 shows the existence of two overlapping DTA peaks at low strontium content ($1/16 < x < 1/8$); these two peaks were overlapped and appeared as one (922 °C) as the strontium content increases ($x > 1/4$). It is interesting to note that the position of the DTA peak at about 970 °C does not change as the mixture composition changes.

Discussions

From combining the data presented in this study, the endothermic DTA and DTG peak temperatures of the solid satire reactions of Pr_6O_{11}, $BaCO_3$, $SrCO_3$, and Co_3O_4 to Sr-doped praseodymium alkaline-earth cobalt oxides

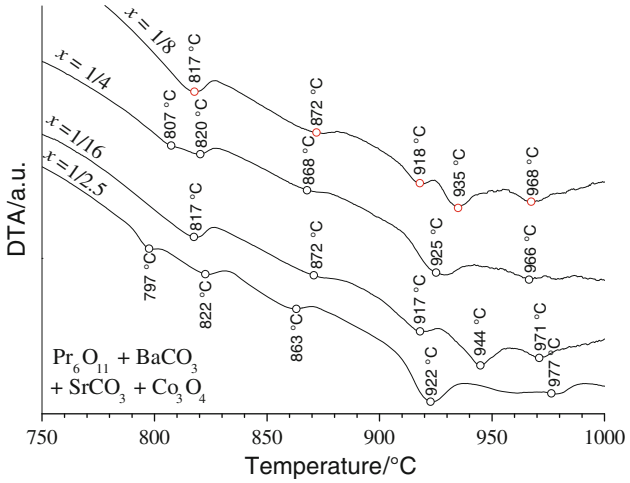

Fig. 6 DTA curves (5 °C/min) obtained from the quaternary mixtures ($x = 1/16$, 1/8, 1/4, and 1/2.5) of Pr_6O_{11}, $BaCO_3$, $SrCO_3$, and Co_3O_4 powders

$PrBa_{1-x}Sr_xCo_2O_{5+d}$ are schematically illustrated in Fig. 7. For instance, from left to right side of Fig. 7 we show our experimental estimation of the DTA thermal events of the single component, binary, ternary ($x = 0.0$) and quaternary ($x = 1/16$, 1/8, 1/4, and 1/2.5) mixtures from the same sequence of events shown in Figs. 1, 2, 4, 5, and 6. For comparison the integrated DTG peaks for Sr-doped praseodymium alkaline-earth cobalt oxides ($x = 0$, 1/16, 1/8, 1/4, and 1/2.5)—as resolved in Fig. 5b—are also schematically shown in right side of Fig. 7.

The following points can be raised from thermal analysis: first three stages (see I–III in Fig. 7) in air atmosphere are quite identical to those found in case of heating the $BaCO_3$, $Ba_{1-x}Sr_xCO_3$ solid solution and Pr_6O_{11}–$BaCO_3$ mixtures. It can be seen that the temperature associated to the $BaCO_3$–$SrCO_3$ mixture increases with increasing of strontium content (x) in I of Fig. 7, whereas the thermal events associated at the first transformation from orthorhombic to hexagonal structure of the $BaCO_3$ do not change as a function of strontium content (x) under the present conditions of mechanical mixture as shown in III of Fig. 7. Within experimental error, the relative temperatures of $Ba_{1-x}Sr_xCO_3$ solid solution system in the Pr_6O_{11}, $BaCO_3$, and Co_3O_4 powder mixture were linear functions (see II in Fig. 7) of the strontium content (x). The values so obtained are in good accord with measurements based on single $BaCO_3$ and $SrCO_3$ components or $Ba_{1-x}Sr_xCO_3$ solid solution and Pr_6O_{11}–$BaCO_3$ mixture (compare with Figs. 1b and 2). Moreover, in comparison with DTA, the DTG peaks of the right side of Fig. 7 are much simpler; changes in DTG peaks in the range temperature 770–820 °C are reasonably correlated with the variations registered in DTA.

With the increasing of temperature, the DTA results of quaternary mixture exhibits a series of peaks at about 870 °C, but these are not associated with any other thermal events, as suggested in IV. Here, it can be also noted that these peaks are centered at the temperature of the broad peak derived from decomposition of Pr_2O_3 (see Figs. 1a and 2) [20].

Both the DTA and DTG peaks (V) shift to higher temperatures with increasing of strontium content (x); whereas the DTA and DTG peaks decreasing with decreasing of barium content ($1-x$), as shown in VI of Fig. 7. Here it can suggest that these two events (V and VI) between about 910 and about 945 °C may be related to decomposition of Co_3O_4, a partial polymorphic transformation of $SrCO_3$ and reaction between Pr_6O_{11} and $SrCO_3$.

In present experimental condition the DTA peaks at about 975 °C—for instance, thermal events detected as VII in Fig. 7—correspond well with the DTG peaks in right side of Fig. 7. In a first approximation, these DTA and DTG peaks were associated with the second polymorphic

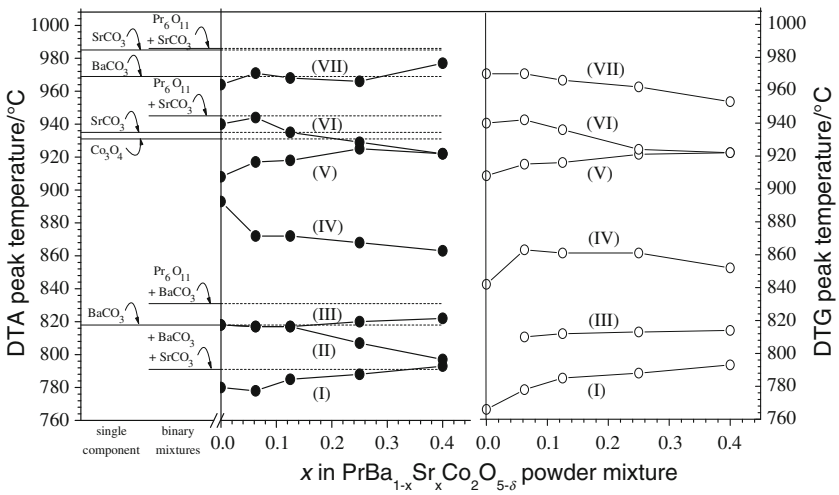

Fig. 7 Plots of DTA and DTG peak temperatures of single, binary, ternary, and quaternary mixtures

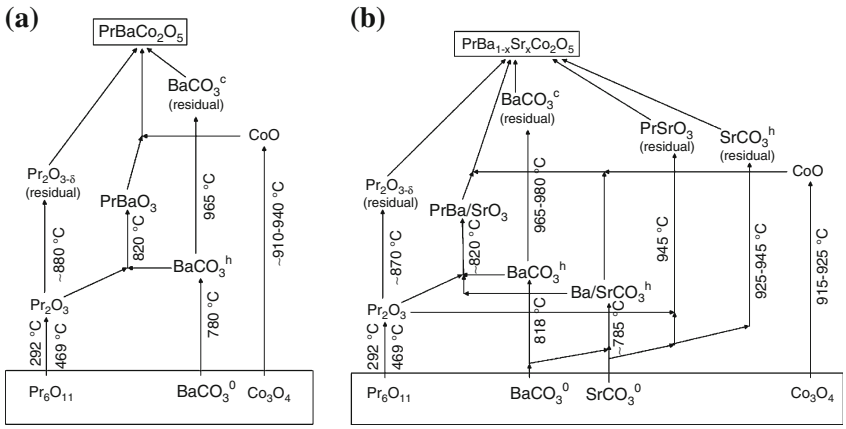

Fig. 8 Schematic representations of the solid-state reaction mechanisms in undoped (**a**) and Sr-doped (**b**) praseodymium alkaline-earth cobalt oxides (x = 1/16, 1/8, 1/4, and 1/2.5)

transformations of $BaCO_3$ from hexagonal into cubic structure.

As reported in the Introduction section, this study was designed to help the elucidation of the solid-state reaction mechanisms from inhomogeneous quaternary (1/16, 1/8, 1/4, and 1/2.5) mixtures of Pr_6O_{11}, $BaCO_3$, $SrCO_3$, and Co_3O_4 powders to Sr-doped praseodymium alkaline-earth cobalt oxides. Certainly, the solid-state reaction between a quaternary powder mixture of oxides (Pr_6O_{11}, Co_3O_4) and carbonates ($BaCO_3$, $SrCO_3$) would appear extremely complex, and traditional techniques such as DTA, TG, or DTG, might help the elucidation of the sequence of single steep reactions involved in high-temperature solid-state reactions [33, 34]. On the basis of the thermal analysis, a tentative reaction sequences from Pr_6O_{11}, $BaCO_3$, $SrCO_3$, and Co_3O_4 powder mixtures to Sr-doped praseodymium alkaline-earth cobalt is proposed. In particular, based on the above discussion, it is evident that (1) the first two thermal events, centered at 292 and 469 °C, are associated with the decomposition of praseodymium sesquiosside to praseodymium (III) oxide and successively reduction to Pr_2O_{3-d} (Eqs. 5 and 6); (2) the competition between the decomposition/reaction of $BaCO_3$ with $SrCO_3$, and $BaCO_3$ with Pr_2O_{3-d} started at relatively intermediate temperature (780–830 °C); (3) $PrBa_{1-x}Sr_xCo_2O_{5+d}$ solid solutions were formed below 980 °C; (4) the strontium content (x) shows remarkable effect on the solid-state reaction and phase transformation; and (5) strontium carbonate in the $BaCO_3$–$SrCO_3$ mixture (i.e., $Ba_{1-x}Sr_xCO_3$ solid solution) can lower the reaction temperature and facilitate the synthesis of $PrBa_{1-x}Sr_xCo_2O_{5+d}$ phase.

The above considerations are schematically summarized in Fig. 8a, b for the undoped and Sr-doped praseodymium alkaline-earth cobalt oxides, respectively. Figure 8 reveal that the precursor powder starts to react at ~300 °C and the reaction develops via a complex process, which runs out at T = 965 °C with the completion of residual $BaCO_3$ decomposition. Moreover, here it can be noted that the

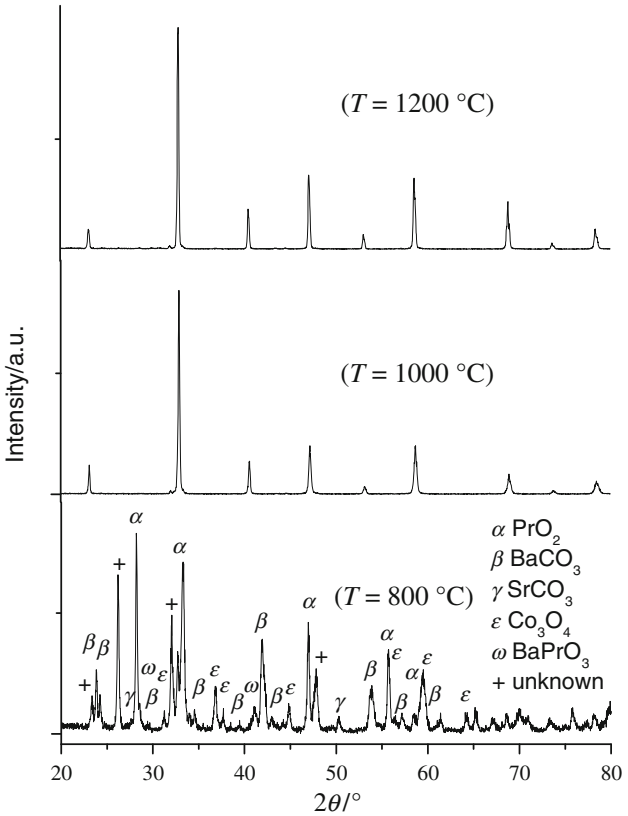

Fig. 9 Representative XRD studies indicating the crystallographic phase evolution for the quaternary mixtures (x = 1/2.5) of Pr_6O_{11}, $BaCO_3$, $SrCO_3$, and Co_3O_4 powders calcined in air at 900, 1000, and 1100 °C for 2 h. Data were collected at room temperature

praseodymium alkaline-earth cobalt oxides compound is mainly produced from the reaction between PrO_2, $\beta BaCO_3$ (or $Ba_{1-x}Sr_xCO_3$ solid solution in the $BaCO_3$–$SrCO_3$ system) and CoO in a temperature range between 780 and 965 °C, as explained in Fig. 8. The final $PrBa_{1-x}Sr_xCo_2O_{5+d}$ phase seems to be formed from the solid-state reaction between CoO and $PrBaO_3$ at a temperature above ~950 °C.

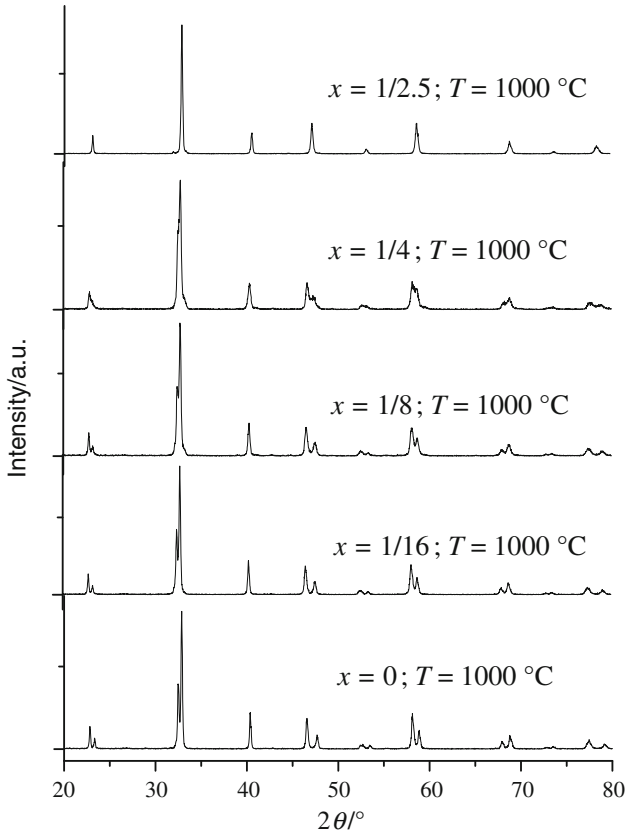

Fig. 10 XRD patterns of products obtained by heating all composition powder precursors, $PrBa_{1-x}Sr_xCo_2O_{5+d}$ ($x = 0$, 1/16, 1/8, 1/4, and 1/2.5) to 1000 °C for 2 h. Data were collected at room temperature

In order to further investigate the reactions taking place during calcinations, and then understand the mechanism of this solid-state reaction clearly, the powder obtained by mixing Pr_6O_{11}, $BaCO_3$, $SrCO_3$, and Co_3O_4 single components was subjected to heat treatments in air at three temperatures ranging from 900 to 1100 °C. The nature of the calcined product was studied by XRD. Figure 9 displays XRD patterns of Sr-doped praseodymium alkaline-earth cobalt oxides with $x = 1/2.5$. XRD studies reveal some important information regarding the phase evolution of the specimens. The X-ray pattern of the heat-treated sample at 900 °C for 2 h is displayed in the bottom of Fig. 9. As we expected, for low reaction temperature, the Bragg reflections of the starting oxides are clearly shown. Moreover, the results obtained from thermal treatment at 900 °C show the presence of additional $PrBaO_3$ and unknown phases, as the minority phases in the XRD pattern. Increasing the sintering temperature to 1000 °C results in appreciable changes in the material, as shown in Fig. 9. This figure displays the X-ray diffractogram for the same sample heat-treated for 2 h at 1000 °C. As the calcination temperature is further increased to 1200 °C, the XRD peaks gradually become sharper and higher, which indicates an increase of crystallinity of the $PrBa_{1-x}Sr_xCo_2O_{5+d}$ phases. In conclusion, calcination temperatures on the range 1000–1100 °C produce well crystallized Sr-doped praseodymium alkaline-earth cobalt oxides, without secondary phases.

Based on the results of XRD for the Sr-doped praseodymium alkaline-earth cobalt oxides with $x = 1/2.5$, 1000 °C was chosen for the calcination temperature all ternary ($x = 0$) and quaternary ($x = 1/16$, 1/8, 1/4, and 1/2.5) mixture precursor to produce $PrBa_{1-x}Sr_xCo_2O_{5+d}$ phases. Figure 10 shows powder XRD patterns of the products obtained by heating the precursor in static air at 1000 °C for 2 h. The XRD analysis indicates that all the obtained compounds are pure with no presence of secondary phases. A second interest of the XRD results is that the overall aspect of the XRD patterns indicates that all the major peaks are split and well separated at low strontium content (x) [13]. Further investigation is necessary to clarify this point, as well as the possible role of the strontium-induced structural effect in $PrBa_{1-x}Sr_xCo_2O_{5+d}$ phases [8, 13, 14].

Conclusions

The solid-state reaction mechanism involved in synthesizing the strontium-doped praseodymium alkaline-earth cobalt oxides solid solution phase is analyzed in this article.

It was found that the formation of $PrBa_{1-x}Sr_xCo_2O_{5+d}$ ($x = 0$, 1/16, 1/8, 1/4, and 1/2.5) solid-state phase by solid-state reaction between non-homogeneity Pr_6O_{11}, $BaCO_3$, $SrCO_3$, and Co_3O_4 powder mixture is a complex process which cannot be described in terms of a single-state reaction model.

Partial substitution of strontium for barium in $PrBa_{1-x}Sr_xCo_2O_{5+d}$ solid solution phase ($x = 0$, 1/16, 1/8, 1/4, and 1/2.5) is found to have a large influence on solid-state reaction mechanisms. Interestingly, it should be noted that the relatively low temperature at which the reaction between $SrCO_3$ and $BaCO_3$ occurs have a strong effect on overall solid-state reaction mechanism.

A qualitative interpretation for the overall progress of the transformation from raw materials has been proposed taking into account the PrO_2, $\beta BaCO_3$, $Ba_{1-x}Sr_xCO_3$ solid solution, $PrBaO_3$, and CoO formation reactions in a temperature range between 780 and 965 °C.

Our results showed that pure phase $PrBa_{1-x}Sr_xCo_2O_{5+d}$ ($x = 0$, 1/16, 1/8, 1/4, and 1/2.5) can be prepared using solid-state reaction at 1000 °C. Moreover, the strontium content characteristics of raw material mixture played an important role also in the synthesized $PrBa_{1-x}Sr_xCo_2O_{5+d}$ solid solution structure ($x = 0$, 1/16, 1/8, 1/4, and 1/2.5).

Acknowledgements This study was supported by a grant (16–2008–04–001–00) from Carbon Dioxide Reduction and Sequestration Research Center, one of the 21st Century Frontier Program funded by the Ministry of Education, Science and Technology of Korean government. The authors are grateful to Dr. Sung Il Jeon, member of our laboratory, for his partial assistance in our studies.

References

1. Nenartaviciene G, Tonsuaadu K, Jasaitis D, Beganskiene A, Kareiva A. Preparation and characterization of superconducting $YBa_2(Cu_{1-x}Cr_x)_4O_8$ oxides by thermal analysis. J Thermal Anal Calorim. 2007;90:173–8.
2. Roy M, Dave P, Barbar SK, Jangid S, Phase DM, Awasth AM. X-ray, SEM, and DSC studies of ferroelectric $Pb_{1-X}Ba_XTiO_3$ ceramics. J Therm Anal Calorim. 2010;101:833–7.
3. Caneiro A, Mogni L, Grunbaum N, Prado F. Physicochemical properties of non-stoichiometric oxides mixed conductors: part I. J Therm Anal Calorim. 2011;103:597–606.
4. Zhang K, Ge L, Ran R, Shao Z, Liu S. Synthesis, characterization and evaluation of cation-ordered $LnBaCo_2O_{5+\delta}$ as materials of oxygen permeation membranes and cathodes of SOFCs. Acta Mater. 2008;56:4876–89.
5. Maignan A, Martin C, Pelloquin D, Nguyen N, Raveau B. Structural and magnetic studies of ordered oxygen-deficient perovskites $LnBaCo_2O_{5+\delta}$, closely related to the 112 structure. J Solid State Chem. 1999;142:247–60.
6. Roy S, Dubenko IS, Khan M, Condon EM, Craig J, Ali N. Magnetic properties of perovskite-derived air-synthesized $RBaCo_2O_{5+\delta}$ (R = La-Ho) compounds. Phys Rev B. 2005;71:024419–27.
7. Streule S, Podlesnyak A, Sheptyakov D, Pomjakushina E, Stingaciu M, Conder K, Medarde M, Patrakeev MV, Leonidov IA, Kozhevnikov VL, Mesot J. High-temperature order-disorder transition and polaronic conductivity in $PrBaCo_2O_{5.48}$. Phys Rev B. 2006;73:094203–8.
8. McKinlay A, Connor P, Irvine JTS, Zhou W. Structural Chemistry and Conductivity of a Solid Solution of $YBa_{1-x}Sr_xCo_2O_{5+\delta}$. J Phys Chem C. 2007;111:19120–5.
9. Seikh MM, Simon C, Caignaert V, Pralong V, Lepetit MB, Boudin S, Raveau B. New magnetic transitions in the ordered oxygen-deficient perovskite $LnBaCo_2O_{5.50+\delta}$. Chem Mater. 2008;20:231–8.
10. Seikh MM, Raveau B, Caignaert V, Pralong V. Switching from unusual to usual ferromagnetism in 112 $LnBaCo_2O_{5.50\pm\delta}$: by calcium doping. J Magn Magn Mater. 2008;320:2676–81.
11. Tarancón A, Chater MR, Skinner SJ, Hernández F, Kilner JA. Layered perovskites as promising cathodes for Intermediate Temperature SOFCs. J Mater Chem. 2007;17:3175–81.
12. Kim G, Wang S, Jacobson AJ, Reimus L, Brodersen P, Mims CA. Rapid oxygen ion diffusion and surface exchange kinetics in $PrBaCo_2O_{5+x}$ with a perovskite related structure and ordered A cations. J Mater Chem. 2007;17:2500–5.
13. Kim JH, Cassidy M, Irvine JTS, Bae J. Advanced electrochemical properties of $LnBa_{0.5}Sr_{0.5}Co_2O_{5+delta}$ (Ln = Pr, Sm, and Gd) as cathode materials for IT-SOFC. J Electrochem Soc. 2009;156:B682–9.
14. Kim YN, Kim JH, Manthiram A. Effect of Fe substitution on the structure and properties of $LnBaCo_{2-x}Fe_xO_{5+\delta}$ (Ln = Nd and Gd) cathodes. J Power Sour. 2010;195:6411–9.
15. Ding H, Xue X. $PrBa_{0.5}Sr_{0.5}Co_2O_{5+\delta}$ layered perovskite cathode for intermediate temperature solid oxide fuel cells. Electrochim Acta. 2010;55:3812–6.
16. Kimura SI, Arai F, Ikezaw M. Mixed valence of praseodymium oxides. J Electron Spectrosc Relat Phenom. 1996;78:135–8.
17. Sulcova P, Trojan M. Synthesis of $Ce_{1-x}Pr_xO_2$ pigments. Thermochim Acta. 2003;395:251–5.
18. Šulcová P, Trojan M. Thermal analysis of pigments based on CeO_2. J Therm Anal Calorim. 2001;65:399–403.
19. Kumari LS, Rao PP, Koshy P. Red pigments based on CeO_2–MO_2–Pr_6O_{11} (M = Zr and Sn): solid solutions for the coloration of plastics. J Am Ceram Soc. 2010;93:1402–8.
20. Zhang Y, Han K, Yin X, Fang Z, Xu Z, Zhu W. Synthesis and characterization of single-crystalline $PrCO_3OH$ dodecahedral microrods and its thermal conversion to Pr_6O_{11}. J Cryst Growth. 2009;311:3883–8.
21. Fahim RB, Zaki MI, Hussien GAM. Effect of processing parameters on the kinetics of decomposition of certain simple anhydrous carbonates. Powder Technol. 1982;33:161–5.
22. Shaheen WM, Selim MM. Thermal characterization and catalytic properties of the ZnO–Co_3O_4/Al_2O_3 system. Int J Inorg Mater. 2001;3:417–25.
23. Manouchehri I, Kameli P, Salamati H. Facile synthesis of Co_3O_4/CoO nanoparticles by thermal treatment of ball-milled precursors. J Supercond Novel Magn. 2011. doi: 10.1007/s10948-011-1141-5.
24. Tang CW, Wang CB, Chien SH. Characterization of cobalt oxides studied by FT-IR, raman, TPR and TG-MS. Thermochim Acta. 2008;473:68–73.
25. Erné BH, van der Weijden AJ, van der Eerden AM, Jansen JBH, van Miltenburg JC, Oonk HAJ. The system $BaCO_3$ + $SrCO_3$; crystal phase transitions: DTA measurements and thermodynamic phase diagram analysis. Calphad. 1992;16:63–72.
26. Weinbruch S, Büttner H, Rosenhauer M. The orthorhombic-hexagonal phase transformation in the system $BaCO_3$-$SrCO_3$ to pressures of 7000 bar. Phys Chem Minerals. 1992;19:289–97.
27. L'vov BV. Mechanism and kinetics of thermal decomposition of carbonates. Thermochim Acta. 2002;386:1–16.
28. Meng B, Tan Xy, Pang Zb. Synthesis and characteristics of Y-dope $BaPrO_3$ ultrafine powders. Chin J Nonferrous Met. 2007;17:636–41.
29. Lippold B, Herrmann J, Boehnke UC, Börner H, Horn J, Semmelhack HC, Wurlitzer M. Investigations on $BaPrO_3$. Solid State Commun. 1991;79:487–9.
30. Horyn R, Wolcyrz M, Bukowski Z. On the existence of $PrSrO_3$-type phase and its Bi/Pr-substituted solid solution. J Solid State Chem. 1996;124:176–81.
31. Boldyrev VV. Reactivity of solids. J Therm Anal Calorim. 1993;40:1041–62.
32. Galwey AAK. What can we learn about the mechanisms of thermal decompositions of solids from kinetic measurements? J Therm Anal Calorim. 2008;92:967–83.
33. Andreouli C, Tsetsekou A. Synthesis of HTSC Re(Y)$Ba_2Cu_3O_x$ powders: the role of ionic radius. Phys C. 1997;291:274–86.
34. Jiang XP, Zhang JS, Huang JG, Jiang M, Qiao GW, Hu ZQ, Shi CX. Study on solid state reaction process of the $YBa_2Cu_3O_{7-x}$ compound. Mater Lett. 1988;7:250–5.